

ETV6 (TEL1) regulates embryonic hematopoiesis in zebrafish

Parisa Rasighaemi,¹ Sara M.N. Onnebo,² Clifford Liongue,¹ and Alister C. Ward¹

¹School of Medicine, and Strategic Research Centre in Molecular and Medical Research, Deakin University, Geelong; and ²School of Life & Environmental Sciences, Deakin University, Burwood, Victoria, Australia

ABSTRACT

Chromosomal translocations involving fusions of the human *ETV6* (*TEL1*) gene occur frequently in hematologic malignancies. However, a detailed understanding of the normal function of ETV6 remains incomplete. This study has employed zebrafish as a relevant model to investigate the role of ETV6 during embryonic hematopoiesis. Zebrafish possessed a single conserved *etv6* ortholog that was expressed from 12 hpf in the lateral plate mesoderm, and later in hematopoietic, vascular and other tissues. Morpholino-mediated gene knockdown of *etv6* revealed the complex contribution of this gene toward embryonic hematopoiesis. During primitive hematopoiesis, *etv6* knockdown resulted in reduced levels of progenitor cells, erythrocyte and macrophage populations, but increased numbers of incompletely differentiated heterophils. Definitive hematopoiesis was also perturbed, with *etv6* knockdown leading to decreased erythrocytes and myeloid cells, but enhanced lymphopoiesis. This study suggests that ETV6 plays a broader and more complex role in early hematopoiesis than previously thought, impacting on the development of multiple lineages.

Introduction

The *ETV6* (ETS variant 6), also known as *TEL1* (*translocating E26 transforming-specific leukemia 1*), gene encodes a nuclear phosphoprotein belonging to the ETS family of transcription factors, which collectively play important roles in a diverse range of cellular processes, including proliferation, differentiation, apoptosis and transformation.¹ *ETV6* is widely expressed during embryonic development, with higher levels of expression observed in the developing kidney, liver and lung, as well as the cranial nerve ganglia, dorsal root ganglia and the ventral region of the caudal neural tube,² and shows broad expression in the adult, including in various hematopoietic cells.² Like other ETS family members, ETV6 possesses two conserved domains: a PNT (pointed) or HLH (helix-loop-helix) domain at its N-terminus and an ETS domain at its C-terminus, and has been identified as a strong transcriptional repressor.^{3,4} The PNT domain is responsible for both homodimerization and heterodimerization with a range of proteins, including the closely-related ETV7 (TEL2) protein, the ETS family member FLI1 and the ubiquitin-conjugating enzyme UBC90.^{4,6} This domain is required for the repression of target genes,⁵ and also mediates the nuclear export of ETV6, thereby regulating its activity.⁷ The positively charged ETS domain is responsible for binding to purine rich segments of DNA, recognizing a core GGAA/T sequence.⁸ A less conserved central domain contributes to the strong repressional activity of ETV6 through binding of various co-repressors, including mSin3A, SMRT, and N-CoR, which subsequently recruit histone deacetylases to mediate transcriptional repression.^{4,9,10}

The human *ETV6* gene is located in a region on the short arm of chromosome 12 that is notable for its frequent involvement in chromosomal translocations associated with hematologic malignancies. Around 50 different translocations involving *ETV6* have been reported, involving around 30 partner genes.¹¹ Alternate functional domains of ETV6 are represented in these fusions. For example, fusions with

JAK2¹² and RUNX1¹³ involve the PNT domain of ETV6, while MN1 fusions involve the ETS domain.¹⁴ Moreover, diverse molecular mechanisms can contribute to the pathogenesis of leukemia resulting from ETV6 fusion, including mislocalization of partner kinases or functional disruption of partner transcription factors.^{3,9} Interestingly, in many cases, leukemic cells harboring *ETV6* translocations possess no functional ETV6 protein due to deletion of the wild-type *ETV6* allele,^{13,15,16} specific point mutations leading to truncated unstable forms of ETV6,¹⁷ or dominant negative effects of the fusion protein over normal ETV6 function.¹¹ This observation suggests a negative regulatory role for ETV6 within the hematopoietic transcriptional hierarchy, underpinning a likely tumor suppressor function for this protein.

Targeted knockout of *Etv6* in mice resulted in embryonic lethality at the E10.5-11.5 stage of development due to apoptosis of mesenchymal and neural cells and defective yolk sac angiogenesis.² Further analysis using chimeric mice revealed that *Etv6* was essential for the establishment of definitive hematopoiesis in the bone marrow.¹⁸ Consistent with these findings, knockdown of *etv6* in *Xenopus* revealed a requirement for this gene in the formation of the first definitive hematopoietic stem cells in the dorsal aorta.¹⁹ Conditional knockout of *Etv6* in adult mice identified an essential role in survival of adult hematopoietic stem cells (HSCs) within the hematopoietic niches.²⁰ However, ablation of *Etv6* after lineage commitment did not affect adult hematopoiesis, except for specific maturation defects in the megakaryocyte lineage.²⁰ In contrast, transgenic mice expressing human *ETV6* under control of the *Gata1* promoter showed accelerated proliferation of early erythroid progenitors, and increased erythroid differentiation.²¹

Zebrafish is an established model for the study of hematopoiesis, showing broad conservation with mammalian species, including distinct primitive and definitive waves of development.²² Zebrafish primitive hematopoietic progenitors are initially derived from hemangioblasts within the lateral plate mesoderm,²² and express early hematopoietic genes, such

©2015 Ferrata Storti Foundation. This is an open-access paper. doi:10.3324/haematol.2014.104091

The online version of this article has a Supplementary Appendix.

Manuscript received on January 29, 2014. Manuscript accepted on September 29, 2014.

Correspondence: award@deakin.edu.au

as *scl* and *ikaros*.^{23,24} From these progenitors, foci for myeloid (*spi1*) and erythromyeloid (*gata1*, *spi1*) generation are established.^{25,26} Rostrally, macrophage cells expressing *lysozyme* (*lyz*) are produced,²⁷ and caudally there is production of erythroid cells expressing β -*embryonic globin* (β -*e-g*)²⁸ and heterophilic granulocytes expressing *myeloperoxidase* (*mpo*) and *matrix metalloproteinase 9* (*mmp9*).^{29,30} Finally, from the dorsal aorta emerge definitive hematopoietic stem cells (HSCs) expressing *c-myb*.³¹ Following a transient phase within the caudal hematopoietic tissue,³¹ these HSCs seed the developing kidney, which becomes the principal site of hematopoiesis, and the thymus. Here early *ikaros*⁺ lymphoid precursors yield mature *rag1*⁺ T cells.^{24,32}

In previous studies, we and others have shown that zebrafish is susceptible to the effects of the *ETV6-JAK2*^{33,34} and *ETV6-AML1*³⁵ oncogenes, which has validated this organism as a useful model for the study of leukemogenesis as well as *ETV6*. Here we have taken further advantage of this model to investigate the function of *ETV6* during embryogenesis. This has identified several distinct roles for *ETV6* in embryonic hematopoiesis with implications for understanding its role in leukemogenesis.

Methods

Zebrafish maintenance and manipulation

All work involving zebrafish was approved by the Deakin University Animal Ethics Committee. Wild-type zebrafish stocks were maintained using standard husbandry practices, as described.³⁴ Two anti-sense morpholinos (Gene Tools) targeting zebrafish *etv6* were used: a splice-blocking morpholino targeting the exon II/intron II splice junction (SSmo: 5'-ACACAGAAAATGCAGATTACCTTA) and one targeting the 5' untranslated region (UTRmo: 5'-TCTTGTGTTTCCACTTTCCTCTCCT), as well as one targeting the *lycat* gene (5'-CTGAACACACACACTGACCGAAGC),³⁶ and a control scrambled morpholino (Co: 5'-CCTCTTACCTCAGTTACAATTATA). In addition, morpholino-resistant mRNA encoding Flag-tagged *etv6* was generated by *in vitro* transcription, as described.³³ Embryos were microinjected at the 1 cell stage with SSmo (8 fmol) and UTRmo (16 fmol) alone or in combination with the morpholino-resistant *etv6* mRNA (0.6 ng) using finely drawn capillaries, and raised at 28°C in egg water (2.5% (w/v) Na₂HPO₄; pH 6.0-6.3) containing 0.003% (w/v) 1-phenyl-2-thiourea to inhibit pigment formation.

RT-PCR and Q-RT-PCR

Total RNA was isolated from pools of 30 whole wild-type or morphant zebrafish embryos at different developmental time points using TRIzol (Invitrogen), except for *c-myb* analysis when embryos were manually dissected into rostral and caudal segments. The RNA was reverse transcribed to cDNA using an iScript cDNA synthesis kit (Bio-Rad). To confirm the effectiveness of the splice site blocking morpholino, PCR was performed using GoTaq Green Master Mix (Promega) and primers specific for exon 1 (5'-CCGGAAGGTGTTAACCATCG) and exon 3 (5'-GAGGAAGTG-GAGTTTGGCAGTG) of the *etv6* gene. Parallel amplification of the β -*actin* gene was used as a control, as described.³⁷ To quantify the relative expression of key hematopoietic genes, Q-RT-PCR was performed using iQ SYBR Green Supermix (Bio-Rad) and gene-specific primers detailed in *Online Supplementary Table S1*. All reactions were performed with 5 replicates using the Agilent Stratagene MX3000P system, with data analyzed using the Livak method³⁸ and expressed as a fold change normalized to the β -*actin* housekeeping gene, as described.²⁵

WISH and DWISH

Whole-mount *in situ* hybridization (WISH) was performed on dechorionated embryos using digoxigenin (DIG)-labeled anti-sense probes, as described previously,³⁴ with sense probes used in parallel as a negative control. For *etv6*, a probe encompassing the full-length transcript (1657 bp) was used.³³ Double WISH was carried out essentially as described.³⁹ Briefly, embryos were hybridized with an *scl* probe labeled with fluorescein-UTP and a *etv6* probe labeled with DIG-UTP. The *scl* probe was detected first using an anti-fluorescein alkaline phosphatase conjugate (Roche) and Fast Red (Roche) as a substrate. After removing the first antibody with acid treatment (0.1 M glycine-HCl pH 2.2, 0.1% Tween-20), the *etv6* probe was then detected using an anti-DIG alkaline phosphatase conjugate (Roche) and NBT/BCIP (Roche) as a substrate.

Histochemical staining

To detect proliferation, embryos were incubated in 10 mM BrdU (Sigma) in Danieau water at 4°C for 20 min, rinsed and incubated at 28.5°C for 5 min, before staining for BrdU incorporation, as described.⁴⁰ To detect apoptotic cells, embryos were incubated in 5 μ g/mL acridine orange (Sigma) for 20 min, washed 8 times in egg-water and examined immediately under UV light or subjected to staining with anti-caspase 3 (BD Bioscience), as described.⁴⁰

Results

Characterization of teleost *etv6* genes

Consistent with other studies,^{41,42} extensive bioinformatics analyses identified a single *etv6* gene in both zebrafish and pufferfish, with the encoded protein showing high conservation to mammalian *ETV6* proteins, particularly within the PNT and ETS domains where overall identity was more than 80% and more than 90%, respectively (*Online Supplementary Figure S1A*). Teleost *etv6* genes showed conserved splicing (*Online Supplementary Figure S1B*) and synteny (*Online Supplementary Figure S1C*) with human *ETV6*, with the encoded *etv6* proteins forming a clade with other vertebrate *ETV6* proteins, which was distinct from the closely related *ETV7* and *SPDEF* (SAM pointed domain containing ETS transcription factor) (*Online Supplementary Figure S1D*).

Embryonic expression profile of *etv6* gene in zebrafish

To gain further insight into the role of *ETV6* during embryogenesis, the spatio-temporal expression profile of zebrafish *etv6* was investigated by whole-mount *in situ* hybridization using a full-length anti-sense probe. Transcripts of *etv6* were evident in 1 cell embryos (Figure 1A), indicative of maternal derivation. By 12 hpf, this was replaced by zygotic expression restricted to bilateral stripes corresponding to the lateral plate mesoderm (LPM) (Figure 1B), which contains precursors for both blood and vasculature.²² By 18 hpf staining was seen in the LPM-derived anterior lateral mesoderm (ALM), pronephric duct and posterior intermediate cell mass (pICM) (Figure 1C and D), the sites of myeloid and erythromyeloid progenitor production, respectively, during the transient primitive wave of zebrafish hematopoiesis.⁴³ The observed *etv6* expression pattern was similar to that previously described for *scl*.⁴⁴ Therefore, double *in situ* hybridization was performed with probes for both *etv6* and *scl*. This indicated that *etv6* was expressed in a subset of *scl* positive cells at this time point (Figure 1E1-E3). A similar pattern of expression was observed at 24 hpf (Figure 1F), but extending to the nascent

pICM-derived posterior blood island (PBI). From 48 hpf, weak *etv6* expression was detected in the vasculature, particularly the inter-segmental vessels between successive somites, the caudal hematopoietic tissue (CHT), a transient secondary site of hematopoiesis, as well as anteriorly (Figure 1G and H). By 72 hpf, *etv6* expression was mostly anterior, including in the tectum, cerebellum, thymus, as well as in the developing gut and kidney, the latter being the ultimate site of definitive hematopoiesis (Figure 1I-J). This pattern was largely maintained up to 6 dpf, when additional expression was also observed within optic sensory epithelium (Figure 1K). No staining was observed using a sense probe as a control (Figure 1L-N). Blood and vasculature are derived from a common precursor, the hemangioblast,²³ which can be specifically ablated with a morpholino targeting *lycat*.³⁶ Injection of this morpholino resulted in a drastic reduction in the level of both *scl* (Figure 1O and P) and *etv6* (Figure 1Q-T), the latter quantified by Q-RT-PCR at 3.6-fold ($P < 10^{-4}$). This collectively suggests that *etv6* is expressed in hemangioblast-derived cells and

likely participates in zebrafish embryonic development, including hematopoiesis.

Targeted knockdown of zebrafish *etv6*

To investigate the potential involvement of *etv6* during zebrafish embryogenesis, an anti-sense morpholino mediated gene knockdown strategy was used. Two independent morpholinos were used to verify the specificity of the phenotypes observed: one targeting sequences upstream of the *etv6* start codon (UTRmo) and the other targeting the donor splice-site for exon 2 (SSmo) (Figure 1U). RT-PCR using primers for exon 1 and 3 confirmed robust inhibition of splicing in the SSmo-injected embryos (Figure 1V), with Q-RT-PCR quantifying this as a highly significant 10.4-fold decrease ($P < 10^{-14}$). An alternatively-spliced product was also detected, the sequencing of which revealed it to represent a complex splice product with retained intronic sequence and use of an alternate exon, which would encode just the first 12 residues of *etv6*, followed by 35 novel residues before a stop codon (Figure 1W).

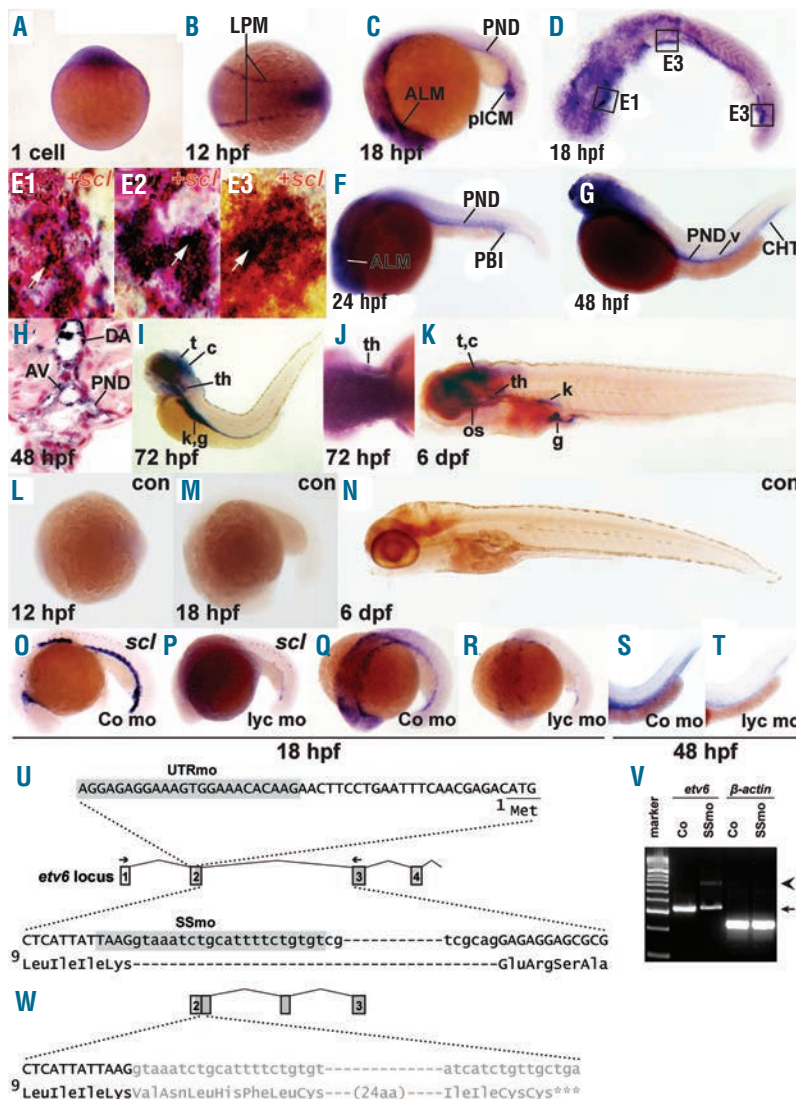


Figure 1. Expression of the zebrafish *etv6* gene during embryonic development and its targeted knockdown using morpholinos. (A-Q) Whole-mount *in situ* hybridization analysis of *etv6* expression. Zebrafish embryos, either wild-type (A-N) or injected with control morpholino (Co mo) (O, Q, S) or *lycat* mo (*lyc mo*) (P, R, T), at the developmental time points indicated. These were hybridized separately with anti-sense *etv6* probes (A-D, F-K, Q-T), control (con) sense *etv6* probes (L-N) or *scl* probes (O-P) with expression evident as blue staining, or co-stained for *scl* (in red) and *etv6* (blue) (E1-E3). (A) Lateral view with the 1 cell to the top; (B, J and L) dorsal views with rostral to the left; (C, F, G, I, K, M-P, S-T) lateral views; (Q-R) oblique lateral views with anterior to the left; and (D and E1-E3) represent dorsal views of flat-mount embryos, the latter representing close-up views of regions equivalent to those boxed in (D), with *etv6* staining indicated with the white arrows, while (H) is a cross-section. LPM: lateral plate mesoderm; ALM: anterior lateral mesoderm; PND: pronephric duct; pICM: posterior intermediate cell mass; PBI: posterior blood island; v: vessels; CHT: caudal hematopoietic tissue; DA: dorsal aorta; AV: axial vein; t: tectum; c: cerebellum; th: thymus; k: kidney; g: gut; os: optic sensory epithelium. (U-W) Morpholino-mediated knockdown of *etv6*. Schematic representation of the zebrafish *etv6* locus (middle) and its targeting with specific anti-sense morpholinos directed to the 5'UTR (UTRmo, upper), and exon 2/intron 2 splice-site (SSmo, lower) (U). Exonic sequence is displayed in upper case and intronic sequence in lower case, with binding sites for morpholinos shaded. The relevant encoded amino acids are shown below with numbering. Arrows show the location of primers used for RT-PCR analysis. RT-PCR analysis of total RNA extracted from SSmo-injected (SSmo) and control (Co) embryos using specific primers for *etv6* and β -actin as indicated (V). The arrow and arrowhead indicate the positions of wild-type and novel *etv6* transcripts, respectively, relative to a size marker. The structure of the alternatively-spliced transcript is shown, including relevant nucleotide and encoded amino acid sequences derived from an extended exon 2 and the use of the alternate exon 1b (W).

Zebrafish *etv6* is involved in primitive hematopoiesis

Examination of embryos injected with either morpholino by light microscopy revealed no overt developmental disruption compared to control embryos, apart from a mild anemia. To further investigate the role of *etv6* during hematopoiesis, specific blood lineage markers were investigated. At 14 hpf, *etv6* and control morphant embryos showed equivalent expression of *scl* (Figure 2A and B), a marker of hemangioblasts,⁴⁵ and *gata1* (Figure 2C-F), an early erythroid marker.²⁶ However, by 20 hpf the *scl* expression pattern was altered in *etv6* morphant embryos, with increased expression rostrally and dorsally (Figure 2G-I, W), but reduced expression in the pICM (Figure 2K-M, X). Both of these phenotypes were able to be rescued by co-injection of morpholino-resistant *etv6* mRNA (Figure 2J, N, W-X). A significant decrease in *gata1* expression was also observed within the pICM at the same time point (Figure 2O-Q, Y),

which could also be rescued (Figure 2R and Y). Finally, β -embryonic globin (β -*e-g*), a late erythroid marker,²⁸ was similarly reduced in morphant embryos (Figure 2S-U, Z). Quantitative RT-PCR (Q-RT-PCR) expression analysis confirmed significantly reduced expression of both *gata1* and β -*e-g*, but also revealed increased expression of *erythropoietin* (*epo*), indicating that defective *epo* signalling was not responsible (Figure 2V).

At 36 hpf, morphant signaling embryos showed significantly increased expression of *gata1* (Figure 3A-C), but β -*e-g* expression (Figure 3D-F) and O-dianisidine staining of hemoglobin (Figure 3G-I) were both decreased. Analysis with Q-RT-PCR confirmed the increased *gata1* and reduced β -*e-g* levels at this time point, with *epo* levels no longer statistically different to controls (Figure 3J). Differential blood cell counts at 48 hpf indicated a statistically-significant increase in pro-erythroblasts (Figure

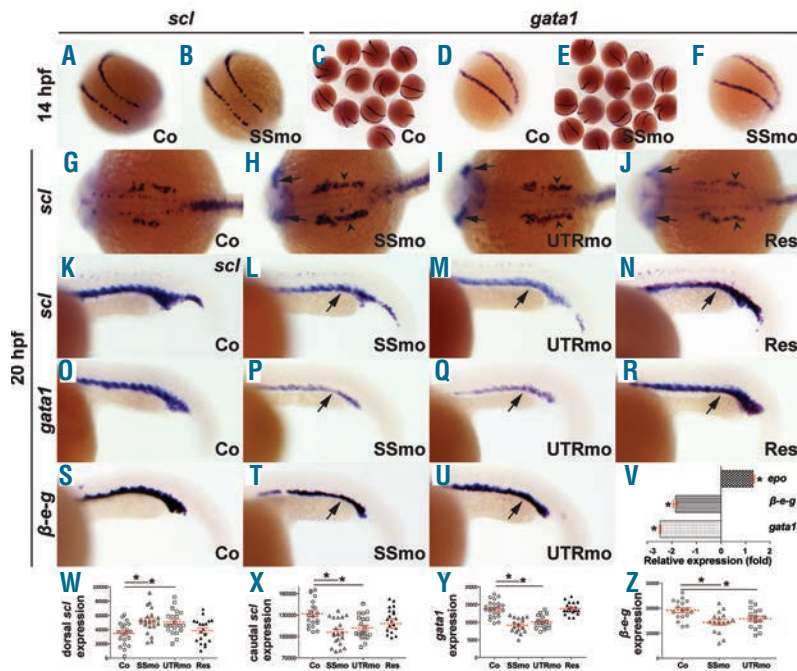


Figure 2. Knockdown of zebrafish *etv6* disrupts primitive hematopoiesis. (A-U, W-Y) WISH analysis of control (Co), morphant (SSmo, UTRmo) and rescued (Res) embryos for expression of *scl* (A-B, G-N, W-X), *gata1* (C-F, O-R, Y), β -*e-g* (S-U, Z) at the times indicated, with quantitation of dorsal *scl* (W), caudal *scl* (X), total *gata1* (Y) and total β -*e-g* (Z) at 20 hpf expressed as mean relative area of expression \pm SEM (*: $P < 0.05$). Regions of altered staining are indicated with the arrows and arrowheads. (V) Q-RT-PCR analysis of RNA extracted from control and SSmo-injected embryos for the expression of *gata1*, β -*e-g* and *epo* at 20 hpf, expressed as mean fold change in morphant relative to control embryos \pm SEM from 5 replicates (*: $P < 0.05$).

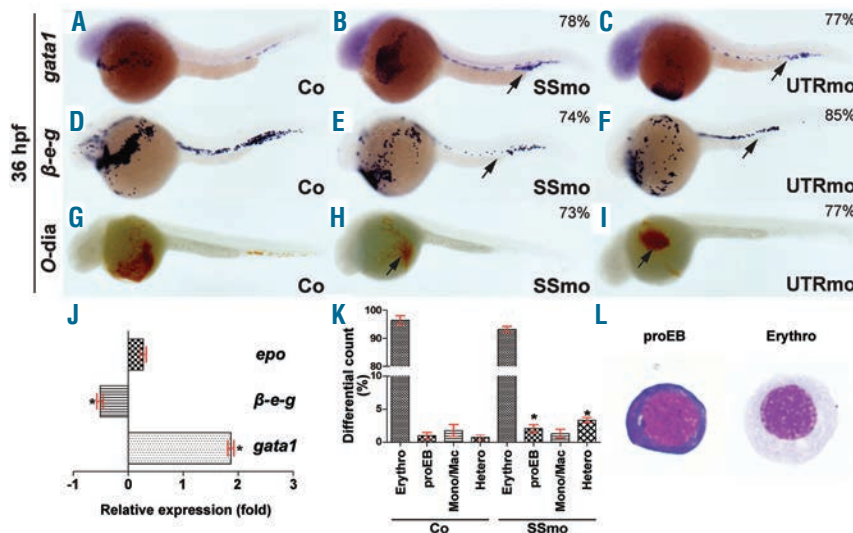


Figure 3. Effect of *etv6* knockdown on erythroid and other blood cells. (A-I) WISH and histochemical analysis of control (Co) and morphant (SSmo, UTRmo) embryos for expression of *gata1* (A-C) and β -*e-g* (D-F) and O-dianisidine staining of hemoglobin (G-I) at 36 hpf, with the proportion of embryos affected shown. (J) Q-RT-PCR analysis of RNA extracted from control and SSmo-injected embryos for the expression of *epo*, β -*e-g* and *gata1* at 36 hpf. (K-L) Analysis of Wright-Giemsa stained blood smears from 48 hpf SSmo-injected and control embryos by differential quantitation (K) and light microscopy (L). Erythro: erythrocytes; proEB: pro-erythroblasts; Mono/Mac: monocyte/macrophages; Hetero: heterophils (*: $P < 0.05$).

3K), but no alterations in morphology were observed (Figure 3L).

The myeloid compartment was examined by analysis of *spi1*, an early pan-myeloid marker,²⁵ *lysozyme* (*lyz*), a marker of early macrophages that develop rostrally and later heterophils,²⁷ and *mmp9*, a marker of various cell populations including heterophils.³⁰ At 14 hpf, *spi1* expression was normal in *etv6* morphants (Figure 4A-D). However, by 20 hpf there was a significant decrease in the number of cells expressing *spi1* (Figure 4E-H) or *lyz* (Figure 4I-L) in the rostral part of the embryo. In contrast, a substantial increase in expression of *mmp9* in the region around the cloaca was observed (Figure 4M-P). Histochemical analysis for myeloperoxidase (Figure 4Q-S), and Sudan Black (Figure 4T-V), which specifically stain heterophils,²⁹ confirmed increased numbers of these cells at 31 hpf. Analysis of blood smears revealed an increased proportion of heterophils in morphants (Figure 3K), although a large proportion of these showed incomplete differentiation (Figure 4W-X).

Zebrafish *etv6* affects definitive hematopoiesis

To explore the role of *etv6* during definitive

hematopoiesis, *etv6* morphants were examined using a range of specific molecular markers. Knockdown of *etv6* led to increased expression of *runx1*⁴⁶ at 36 hpf (Figure 5A-B, I') that reached significance at 48 hpf (Figure 5C-D, I') and *c-myb*³¹ from 36 hpf to 3 dpf (Figure 5E-H, I-K, I'), when *c-myb* positive precursors migrate from the CHT to the thymus. Q-RT-PCR analysis performed separately for the rostral and caudal regions of embryo showed that the increased expression was restricted to the caudal region (Figure 5J'). Conversely, by 5 dpf, *c-myb* was slightly reduced in the CHT, thymus and kidney of morphant embryos (Figure 5L-N, J'), indicative of a disruption of progenitor cells. Morphant embryos were also overtly anemic by light microscopy, which was confirmed by reduced O-dianisidine staining at 4 dpf (Figure 5O-Q) and β -*e-g* expression at 5 dpf (Figure 5U-W, J'). Interestingly, this was despite increased *gata1* at 5 dpf (Figure 5R-T), confirmed by Q-RT-PCR at 5 dpf when *epo* expression was also increased and *epor* expression was normal (Figure 5J'), confirming the reduced erythroid differentiation was not due to defective epo signaling. Morphant embryos maintained significantly increased numbers of circulating pro-erythroblasts (Figure

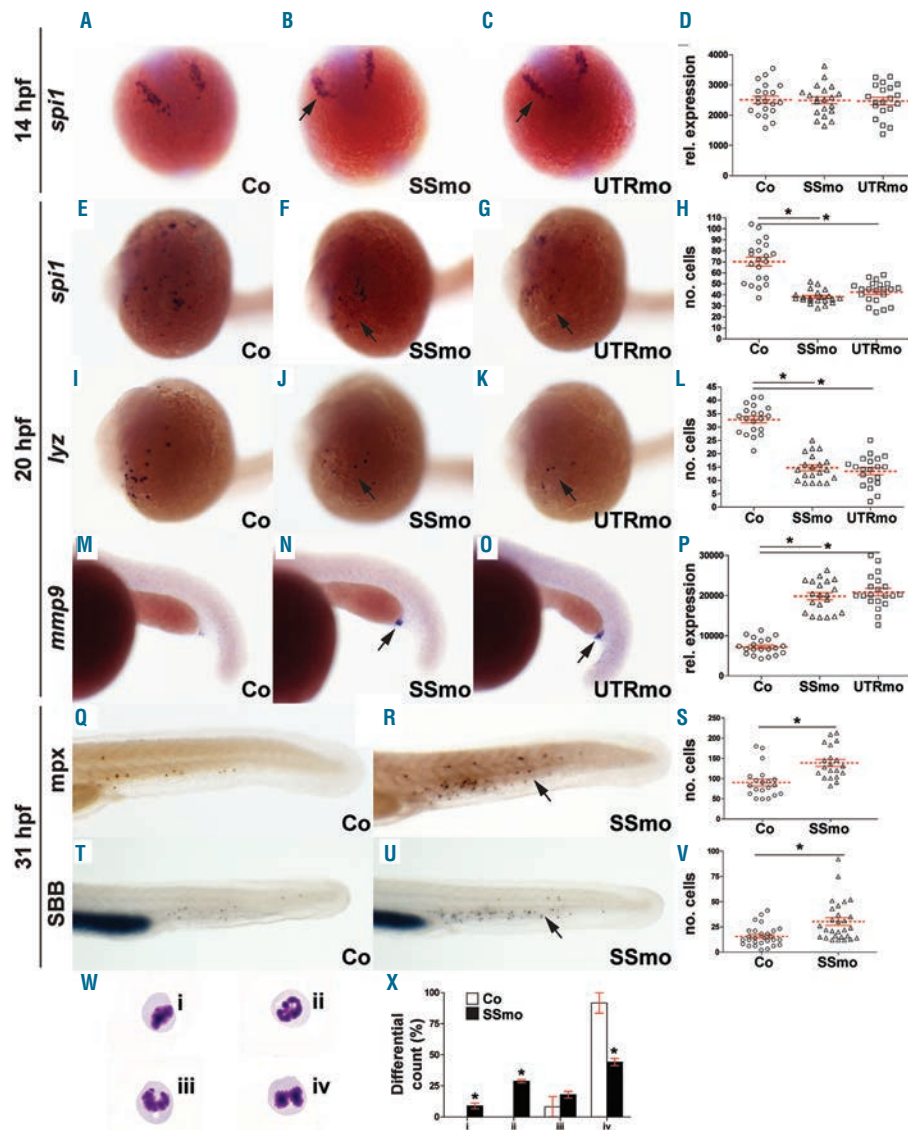


Figure 4. Knockdown of *etv6* disrupts primitive myelopoiesis. (A-P) WISH analysis of morphant and control embryos for expression of *spi1* at 14 hpf (A-D) and 20 hpf (E-H), *lyz* and *mmp9* at 20 hpf (I-L and M-P, respectively), with quantitation of relative expression area of *spi1* at 14 hpf (D), the number of positive cells for *spi1* and *lyz* expression at 20 hpf (H and L, respectively) and expression area of *mmp9* at 20 hpf (P), presented as mean \pm SEM (*: $P < 0.05$). (Q-V) Histochemical staining for myeloperoxidase activity (mpx) (Q-S) and Sudan Black B (SBB) (T-V) at 31 hpf on SSmo-injected and control embryos, with the number of positive cells presented as mean \pm SEM (S and V, respectively) (*: $P < 0.05$). (W-X) Morphological characterization of heterophil differentiation observed in 48 hpf blood smears by light microscopy (W: i-iv), and their quantitation in SSmo injected and control embryos (X).

5K'-L'), although these are largely derived from primitive erythropoiesis at this time point.⁴⁷ Analysis of BrdU incorporation revealed increased proliferation within the CHT at 3 dpf (Figure 5X-B'), whereas staining with acridine orange (Figure 5C' and D') and anti-caspase 3 (Figure 5E'-H') indicated enhanced apoptosis in this region at 4-5 dpf.

To examine the role of *etv6* in definitive myeloid cell development, the myeloid specific markers, *lyz* and *mmp9*, were also examined at 5 dpf. Interestingly, morphant embryos showed a modest expansion of *lyz*⁺ cells (Figure 6A-C, E), which could be rescued by co-injection of morpholino-resistant *etv6* mRNA (Figure 6D and E). In contrast,

there was a reduction of *mmp9*⁺ cells (Figure 6F-I), with this differential effect confirmed by Q-RT-PCR analysis of the respective genes (Figure 6W). Blood examination at 5 dpf revealed elevated numbers of monocyte/macrophages in morphant embryos compared to controls, while in contrast circulating heterophils were lessened in morphants, although this did not reach significance (Figure 5K' and L'). Finally, lymphopoiesis was investigated through evaluation of the lymphoid markers *ikaros*²⁴ and *rag1*.³² In *etv6* morphant embryos expression of *ikaros* was increased at 3 dpf (Figure 6J-M) and 5 dpf (Figure 6N-Q). Expression of the late lymphoid marker *rag1* was also increased at 5 dpf (Figure

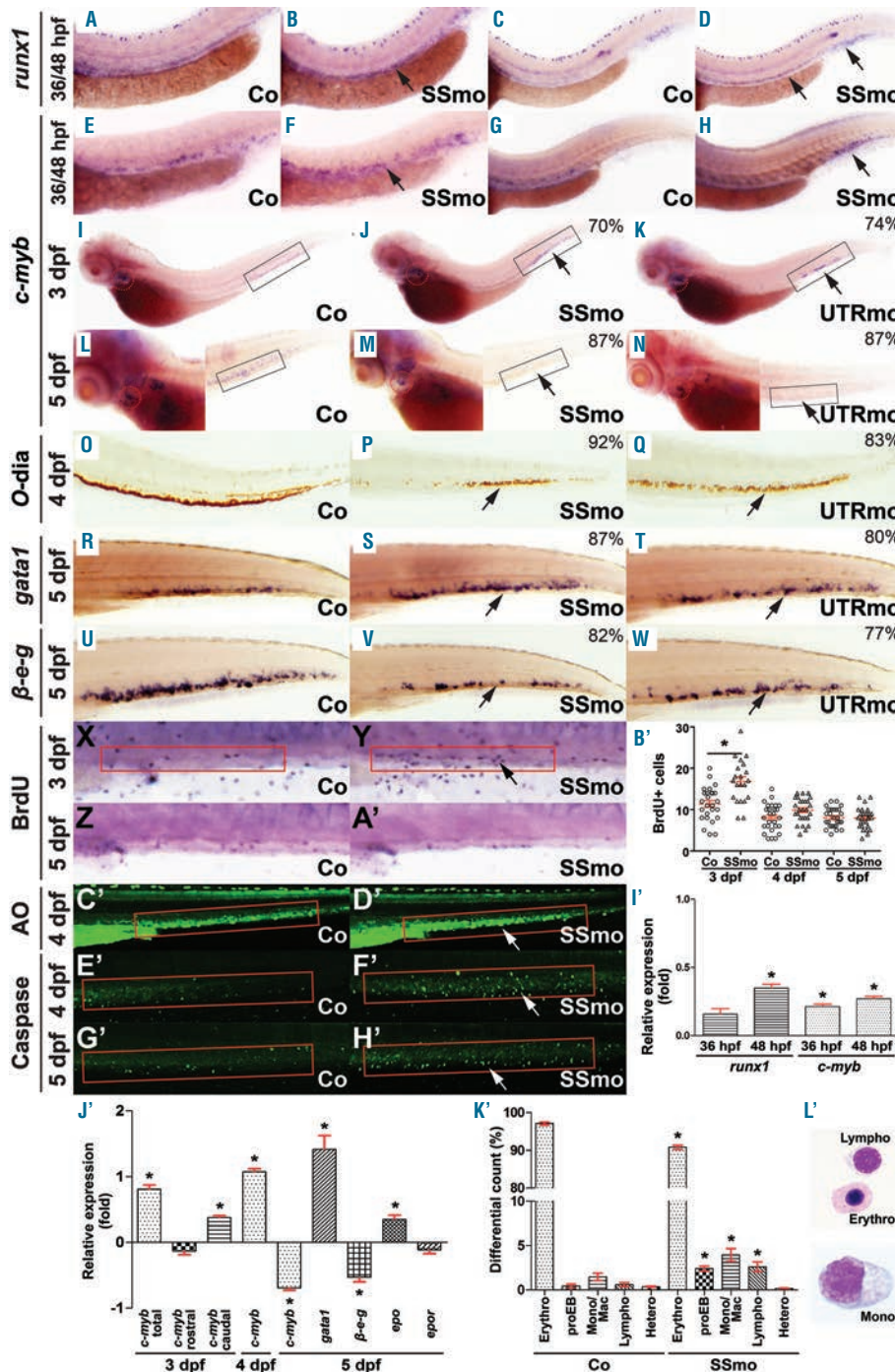


Figure 5. Knockdown of *etv6* affects definitive HSC and erythroid compartments. (A-N, R-W) WISH analysis of the indicated morphant and control embryos for the expression of *runx1* at 36 hpf (A-B) and 48 hpf (C-D), *c-myb* at 36 hpf (E-F), 48 hpf (G-H), 3 dpf (I-K) and 5 dpf (L-N), *gata1* (R-T) and β -e-g (U-W) at 5 dpf. (O-Q, X-F) Histochemical staining of the indicated morphant and control embryos to detect hemoglobin using O-dianisidine hemoglobin (O-dia) (O-Q), proliferation using BrdU incorporation (X-B') and apoptosis using acridine orange (AO) (C'-D') and anti-caspase 3 (E'-H') at the times shown, with the number of BrdU-positive cells \pm SEM shown (B'). (I'-J) Q-RT-PCR analysis of *runx1* and *c-myb* at 36 hpf and 48 hpf, total (I'), and rostral and caudal *c-myb* at 3 dpf, total *c-myb* at 4 dpf, and *c-myb*, *gata1*, *epo* and *epor* at 5 dpf (J'), expressed as fold change in SSmo-injected relative to control embryos \pm SEM from 5 replicates (*: $P < 0.05$). (K'-L') Analysis of Wright-Giemsa stained blood smears from 5 dpf morphant and control embryos by differential quantitation (K') and light microscopy (L'); designations as described for Figure 3K, with the addition of Lympho (lymphocytes) (*: $P < 0.05$).

6R-T, V), with this phenotype able to be rescued by morpholino-resistant *etv6* mRNA (Figure 6U and V). The increased expression of lymphoid genes in morphants was confirmed by Q-RT-PCR analysis (Figure 6X). In addition, morphant embryos showed higher lymphocyte numbers in peripheral blood smears at 5 dpf (Figure 5K' and L). Moreover, no difference was observed in expression of the thymic epithelium marker *foxn1* (Figure 6Y and Z). This collectively indicates enhanced lymphopoiesis in *etv6* morphants.

Discussion

Despite the frequent involvement of the *ETV6* gene in hematologic malignancies, much remains to be learned about the role of ETV6 during normal hematopoietic development. This is partly related to the embryonic lethality of *Etv6*-knockout mice due to a failure in angiogenesis,^{2,20} which has complicated more detailed studies. Since embryonic development in zebrafish is not dependent on vasculogenesis, we hypothesized that this organism would be a useful alternative vertebrate model for investigating the function of *ETV6* during embryogenesis. This study has characterized the zebrafish *etv6* gene, and delineated its role during embryonic hematopoiesis,

where it acts at multiple levels to influence the production of blood and immune cells.

In agreement with other work,^{41,42} bioinformatic analysis revealed that the zebrafish possessed a single *etv6* protein with high sequence homology with other vertebrate ETV6 proteins, especially within the PNT and ETS domains, indicating functional conservation. Expression studies showed zebrafish *etv6* transcripts were found to be initially maternally-derived, with specific zygotic expression evident from 12 hpf in the LPM in a subset of *scl* positive hemangioblasts.²² By 18 hpf, expression was seen in the anterior lateral mesoderm (ALM) and posterior intermediate cell mass (pICM), the sites of primitive myelopoiesis and erythropoiesis,⁴³ and by 24 hpf staining was also observed in the nascent posterior blood island (PBI), and later in vessels. At 3 dpf, *etv6* expression was evident in the thymus, the site of lymphopoiesis, and later in the developing kidney, the site of definitive hematopoiesis. Expression was drastically reduced in embryos in which hemangioblasts were ablated. This is consistent with the expression studies in *Xenopus*,¹⁹ mice¹⁸ and in various hematopoietic cell lines,¹⁸ suggesting a conserved role in blood and immune cell development across vertebrates. Expression also overlapped with that for the related *etv7* gene.⁴⁸

The earliest zebrafish hematopoietic cells are derived from hemangioblasts in the LPM at 12 hpf,²² characterized

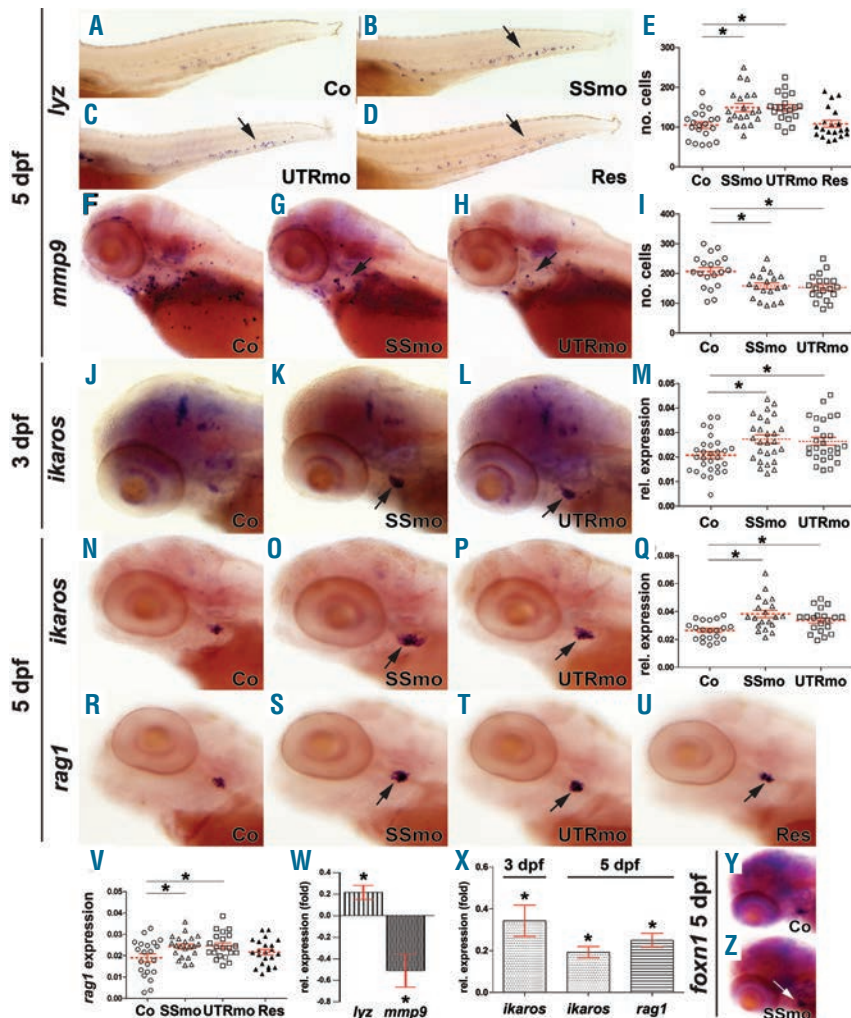


Figure 6. Knockdown of *etv6* affects definitive myeloid and lymphoid compartments. (A-V, Y-Z) WISH analysis of control, morphant and rescued embryos showing representative expression of *lyz* in the tail (A-E) and *mmp9* in the tail (F-I) at 5 dpf, as well as *ikaros* at 3 dpf (J-M) and 5 dpf (N-Q), *rag1* at 5 dpf (R-V), and *foxn1* at 5 dpf (Y-Z) in the thymus. The total number of *lyz*⁺ and *mmp9*⁺ cells in the embryos are presented as mean ± SEM (E and I, respectively), and the area of *ikaros* and *rag1* staining quantified relative to eye size, and expressed as mean ± SEM (M, Q and U, respectively) (*: *P*<0.05). (W-X) Q-RT-PCR analysis of morphant and control embryos for the expression of *mmp9* and *lyz* at 5 dpf (W) or *ikaros* and *rag1* at 3 or 5 dpf as indicated (X), expressed as fold change in SSmo-injected relative to control embryos ± SEM from 5 repeats (*: *P*<0.05).

by the expression of markers for hematopoietic progenitors, such as *scl*, as well as those for early myeloid (*spi1*) and erythroid (*gata1*) populations.^{23,25,26} Morpholino-mediated knockdown of *etv6* did not alter the expression of early hematopoietic markers, suggesting that hematopoietic cell specification was *etv6*-independent. However, at 20 hpf there was differential effect on *scl* populations, with an increase within ventral, non-hematopoietic tissue, but a reduction of caudal expression in hematopoietic tissue, suggesting that *etv6* may influence the early hematopoietic progenitor compartment. This would potentially explain the reduced levels of early (*spi1*) and late (*lyz*) myeloid cells rostrally, and reduced early (*gata1*) and late (β -*e-g*) erythroid cells caudally. Interestingly, there was a specific increase in the *mmp9*⁺ cells caudally, suggesting that *etv6* might also influence lineage choice during primitive hematopoiesis in this region. This is the first study demonstrating the involvement of ETV6 during primitive hematopoiesis, and is in contrast with previous studies that have reported unaffected yolk sac and fetal liver hematopoiesis in *Etv6*^{-/-} mice,^{2,20} which may represent a genuine difference between the two species.

Definitive HSCs in zebrafish originate in the dorsal aorta and migrate first to the CHT before seeding the kidney and thymus.⁴⁷ Morphant embryos showed a significant increase in cells expressing *runx1* and *c-myb* within the dorsal aorta and CHT, which correlated with increased proliferation in the latter. However, by 5 dpf, *etv6* morphants showed an overall decrease in *c-myb* expression, along with increased apoptosis in this region, suggesting *etv6* may impact on cell survival. This is consistent with the failure of *Etv6*^{-/-} progenitors to contribute to bone marrow hematopoiesis in chimeric mouse,¹⁸ and the loss of bone marrow HSCs in mice with *Etv6* specifically inactivated in the hematopoietic compartment.²⁰ Interestingly, *etv6* morphant *Xenopus* embryos exhibited a more severe phenotype, with HSCs completely ablated, although this was secondary to a severe defect in artery formation.¹⁹ An increase in lymphopoiesis was also observed in zebrafish *etv6* morphants concomitant with the loss of *c-myb*⁺ cells, suggesting that *etv6*-deficiency may result in preferential differentiation down this lineage. This observation may be of clinical relevance, providing one possible explanation for the high propensity of ETV6 fusions in lymphoid malignancies.

The role of ETV6 in erythropoiesis has remained controversial. Previous work has shown that selective excision of *Etv6* in the erythroid lineage of mice failed to impact on erythropoiesis.²⁰ However, other data have demonstrated that overexpression of ETV6 enhanced erythroid differentiation in cell models,⁴⁹ as well as leading to increased erythroid precursors, accelerated differentiation and augmented globin expression in mice transgenic for *ETV6*.²¹ Our data are consistent with the latter studies, with *etv6* morphants showing an initial decrease in *gata1* expression, followed by a sustained increase in expression. However, despite this increase in early erythroid cells (and a parallel induction of *epo*) *etv6* morphants remained anemic, with decreased β -*e-g*

expression and increased erythroblasts in the blood. This collectively suggests a role for *etv6* in the regulation of red blood cell maturation. Expression of *etv7*, which also contributes to red blood cell maturation,⁴⁸ was reduced in *etv6* morphants. This suggests the two genes may act co-ordinately in this process.

Our data also revealed that *etv6* influences the differentiation of zebrafish heterophils, the piscine neutrophil equivalent. Morphant embryos showed incomplete heterophil differentiation at 48 hpf and reduced numbers of *mmp9*⁺ heterophils at 5 dpf. Close examination of the published study using chimeric mice revealed that while *Etv6*^{-/-} cells were able to contribute to all definitive hematopoietic lineages, the granulocyte/macrophage lineage was under-represented,¹⁸ and the study on the hematopoietic-specific disruption of *Etv6* described reduced neutrophils, despite normal red cell and lymphocyte numbers.²⁰ A role for ETV6 in regulating myeloid differentiation might also be relevant in the context of ETV6 fusions in myeloid malignancies.

Finally, ETV6 has been implicated in angiogenesis, with yolk sac angiogenesis disrupted in *Etv6*^{-/-} mice,² and arterial differentiation ablated in *etv6* morphant *Xenopus* embryos due to loss of VEGFA expression.¹⁹ A more subtle defect was recently reported following *etv6* knockdown in zebrafish embryos, with aberrant trajectories and stalled sprouts observed during intersegmental vessel (ISV) formation.⁵⁰ To verify this, *etv6* SSmo was injected into *flk1:gfp* transgenic embryos, which resulted in similar subtle ISV defects (Online Supplementary Figure S2A-C), confirming this distinct angiogenic role, which may be an indirect consequence of the altered *scl* expression seen in *etv6* morphants. No other vascular defects were observed (*data not shown*). Moreover, overexpression of *etv6* had no significant effect on circulation (Online Supplementary Figure S2D). Collectively, our data suggest that ETV6 participates in both blood and, to a lesser extent, vessel development, consistent with their common derivation from the hemangioblast, and the expression of ETV6 in both lineages.

Funding

The authors acknowledge support from the Deakin University International Research Scholarship scheme (PR, SMNO) and Alfred Deakin Postdoctoral Research Fellow scheme (CL), and access to the resources of FishWorks: Collaborative Infrastructure for Zebrafish Research, an Australian Research Council LIEF initiative (ACW).

Acknowledgments

The authors would like to thank the Deakin University Upper Animal House staff for their assistance with zebrafish husbandry, as well as Dr. Daniel McCulloch and Dr. Yann Gibert for helpful discussions.

Authorship and Disclosures

Information on authorship, contributions, and financial & other disclosures was provided by the authors and is available with the online version of this article at www.haematologica.org

References

- Oikawa T, Yamada T. Molecular biology of the Ets family of transcription factors. *Gene*. 2003;303(1):11-34.
- Wang LC, Kuo A, Fujiwara Y, Gilliland DG, Golub TR, Orkin SH. Yolk sac angiogenic defects and intra-embryonic apoptosis in mice lacking the Ets-related factor TEL. *EMBO J*. 1997;16(14):4374-83.
- Golub TR, McLean T, Stegmaier K, Carroll M, Tomasson M, Gilliland DG. The TEL gene and human leukemia. *Biochim Biophys Acta*. 1996;1288(1):M7-10.
- Chakrabarti SR, Nucifora G. The leukemia-

- associated gene TEL encodes a transcription repressor which associates with SMRT and mSin3A. *Biochem Biophys Res Commun.* 1999;264(3):871-7.
5. Kim CA, Phillips ML, Kim W, Gingery M, Tran HH, Robinson MA, et al. Polymerization of the SAM domain of TEL in leukemogenesis and transcriptional repression. *EMBO J.* 2001;20(15):4173-82.
 6. Potter MD, Buijs A, Kreider B, van Rompaey L, Grosveld GC. Identification and characterization of a new human ETS-family transcription factor, TEL2, that is expressed in hematopoietic tissue and can associate with TEL1/ETV6. *Blood.* 2000;95(11):3341-8.
 7. Wood LD, Irvin BJ, Nucifora G, Luce KS, Hiebert SW. Small ubiquitin-like modifier conjugation regulates nuclear export of TEL, a putative tumor suppressor. *Proc Natl Acad Sci USA.* 2003;100(6):3257-62.
 8. Poirel H, Oury C, Carron C, Duprez E, Laabi Y, Tsapis A, et al. The TEL gene products: nuclear phosphoproteins with DNA binding properties. *Oncogene.* 1997; 14(3):349-57.
 9. Guidez F, Petrie K, Ford AM, Lu H, Bennett CM, MacGregor A, et al. Recruitment of the nuclear receptor corepressor N-CoR by TEL moiety of the childhood leukemia-associated TEL-AML1 oncoprotein. *Blood.* 2000;96(7):2557-60.
 10. Wang L, Hiebert SW. TEL contacts multiple co-repressors and specifically associates with histone deacetylase-3. *Oncogene.* 2001;20(28):3716-25.
 11. De Braekeleer E, Douet-Guilbert N, Morel F, Le Bris M-J, Basinko A, De Braekeleer M. ETV6 fusion genes in hematological malignancies: A review. *Leuk Res.* 2012;36(8): 945-61.
 12. Peeters P, Raynaud SD, Cools J, Wlodarska I, Grosgeorge J, Philip P, et al. Fusion of TEL, the ETS-variant gene 6 (ETV6), to the receptor-associated kinase JAK2 as a result of t(9;12) in a lymphoid and t(9;15;12) in a myeloid leukemia. *Blood.* 1997;90(7): 2535-40.
 13. Golub TR, Barker GF, Bohlander SK, Hiebert SW, Ward DC, Bray-Ward P, et al. Fusion of the TEL gene on 12p13 to the AML1 gene on 21q22 in acute lymphoblastic leukemia. *Proc Natl Acad Sci USA.* 1995; 92(11):4917-21.
 14. Buijs A, Sherr S, van Baal S, van Bezouw S, van der Plas D, van Kessel GA, et al. Translocation (12; 22)(p13; q11) in myeloproliferative disorders results in fusion of the ETS-like TEL gene on 12p13 to the MN1 gene on 22q11. *Oncogene.* 1995; 10(8):1511-9.
 15. Patel N, Goff LK, Clark T, Ford AM, Foot N, Lillington D, et al. Expression profile of wild-type ETV6 in childhood acute leukaemia. *Br J Haematol.* 2003;122(1):94-8.
 16. Raynaud S, Cave H, Baens M, Bastard C, Cacheux V, Grosgeorge J, et al. The 12;21 translocation involving TEL and deletion of the other TEL allele: two frequently associated alterations found in childhood acute lymphoblastic leukemia. *Blood.* 1996;87(7): 2891-9.
 17. Barjesteh van Waalwijk van Doorn-Khosravani S, Spensberger D, de Knegt Y, Tang M, Lowenberg B, Delwel R. Somatic heterozygous mutations in ETV6 (TEL) and frequent absence of ETV6 protein in acute myeloid leukemia. *Oncogene.* 2005; 24(25):4129-37.
 18. Wang LC, Swat W, Fujiwara Y, Davidson L, Visvader J, Kuo F, et al. The TEL/ETV6 gene is required specifically for hematopoiesis in the bone marrow. *Genes Dev.* 1998; 12(15):2392-402.
 19. Ciau-Uitz A, Pinheiro P, Gupta R, Enver T, Patient R. Tel1/ETV6 specifies blood stem cells through the agency of VEGF signaling. *Dev Cell.* 2010;18(4):569-78.
 20. Hock H, Meade E, Medeiros S, Schindler JW, Valk PJ, Fujiwara Y, et al. Tel/Etv6 is an essential and selective regulator of adult hematopoietic stem cell survival. *Genes Dev.* 2004;18(19):2336-41.
 21. Eguchi-Ishimae M, Eguchi M, Maki K, Porcher C, Shimizu R, Yamamoto M, et al. Leukemia-related transcription factor TEL/ETV6 expands erythroid precursors and stimulates hemoglobin synthesis. *Cancer Sci.* 2009;100(4):689-97.
 22. Davidson AJ, Zon LI. The 'definitive' (and 'primitive') guide to zebrafish hematopoiesis. *Oncogene.* 2004; 23(43): 7233-46.
 23. Patterson LJ, Gering M, Eckfeldt CE, Green AR, Verfaillie CM, Ekker SC, et al. The transcription factors Scl and Lmo2 act together during development of the hemangioblast in zebrafish. *Blood.* 2007;109(6):2389-98.
 24. Willett CE, Kawasaki H, Amemiya CT, Lin S, Steiner LA. Ikaros expression as a marker for lymphoid progenitors during zebrafish development. *Dev Dyn.* 2001;222(4):694-8.
 25. Lieschke GJ, Oates AC, Paw BH, Thompson MA, Hall NE, Ward AC, et al. Zebrafish SPI-1(PU.1) marks a site of myeloid development independent of primitive erythropoiesis: implications for axial patterning. *Dev Biol.* 2002;246(2):274-95.
 26. Long Q, Meng A, Wang H, Jessen JR, Farrell MJ, Lin S. GATA-1 expression pattern can be recapitulated in living transgenic zebrafish using GFP reporter gene. *Development.* 1997;124(20):4105-11.
 27. Liu F, Wen Z. Cloning and expression pattern of the lysozyme C gene in zebrafish. *Mech Dev.* 2002;113(1):69-72.
 28. Brownlie A, Hersey C, Oates AC, Paw BH, Falick AM, Witkowska HE, et al. Characterization of embryonic globin genes of the zebrafish. *Dev Biol.* 2003;255(1):48-61.
 29. Lieschke GJ, Oates AC, Crowhurst MO, Ward AC, Layton JE. Morphologic and functional characterization of granulocytes and macrophages in embryonic and adult zebrafish. *Blood.* 2001;98(10):3087-96.
 30. Yoong S, O'Connell B, Soanes A, Crowhurst MO, Lieschke GJ, Ward AC. Characterization of the zebrafish matrix metalloproteinase 9 gene and its developmental expression pattern. *Gene Expr Patterns.* 2007;7(1-2):39-46.
 31. Murayama E, Kissa K, Zapata A, Mordelet E, Briolat V, Lin H-F, et al. Tracing hematopoietic precursor migration to successive hematopoietic organs during zebrafish development. *Immunity.* 2006;25(6):963-75.
 32. Willett CE, Cherry JJ, Steiner L. Characterization and expression of the recombination activating genes (rag1 and rag2) of zebrafish. *Immunogenetics.* 1997;45(6):394-404.
 33. Onnebo SMN, Condron MM, McPhee DO, Lieschke GJ, Ward AC. Hematopoietic perturbation in zebrafish expressing a tel-jak2a fusion. *Exp Hematol.* 2005;33(2):182-8.
 34. Onnebo SM, Rasighaemi P, Kumar J, Liongue C, Ward AC. Alternate TEL-JAK2 fusions associated with T cell acute lymphoblastic leukemia and atypical chronic myelogenous leukemia dissected in zebrafish. *Haematologica.* 2012;97(12): 1895-903.
 35. Sabaawy HE, Azuma M, Embree LJ, Tsai HJ, Starost MF, Hickstein DD. TEL-AML1 transgenic zebrafish model of precursor B cell acute lymphoblastic leukemia. *Proc Natl Acad Sci USA.* 2006;103(41):15166-71.
 36. Xiong JW, Yu Q, Zhang J, Mably JD. An acyltransferase controls the generation of hematopoietic and endothelial lineages in zebrafish. *Circ Res.* 2008;102(9):1057-64.
 37. O'Sullivan LA, Noor SM, Trengove MC, Lewis RS, Liongue C, Sprigg NS, et al. Suppressor of cytokine signaling 1 regulates embryonic myelopoiesis independently of its effects on T cell development. *J Immunol.* 2011;186(8):4751-61.
 38. Livak KJ, Schmittgen TD. Analysis of relative gene expression data using real-time quantitative PCR and the 2- $\Delta\Delta$ CT method. *Methods.* 2001;25(4):402-8.
 39. Jowett T. Double in situ hybridization techniques in zebrafish. *Methods.* 2001;23(4):345-58.
 40. Verduzco D, Amatruza JF. Analysis of cell proliferation, senescence and cell death in zebrafish embryos. *Meth Cell Biol.* 2011; 1011-19.
 41. Montpetit A, Sinnott D. Comparative analysis of the ETV6 gene in vertebrate genomes from pufferfish to human. *Oncogene.* 2001;20(26):3437-42.
 42. Liu F, Patient R. Genome-wide analysis of the zebrafish ETS family identifies three genes required for hemangioblast differentiation or angiogenesis. *Circ Res.* 2008; 103(10):1147-54.
 43. Bertrand JY, Kim AD, Violette EP, Stachura DL, Cisson JL, Traver D. Definitive hematopoiesis initiates through a committed erythromyeloid progenitor in the zebrafish embryo. *Development.* 2007;134(23):4147-56.
 44. Gering M, Rodaway ARF, Gottens B, Patient R, Green AR. The SCL gene specifies haemangioblast development from early mesoderm. *EMBO J.* 1998;17(14):4029-45.
 45. Liao EC, Paw BH, Oates AC, Pratt SJ, Postlethwait JH, Zon LI. SCL/Tal-1 transcription factor acts downstream of cloche to specify hematopoietic and vascular progenitors in zebrafish. *Genes Dev.* 1998;12(5): 621-6.
 46. Lam EY, Hall CJ, Crosier PS, Crosier KE, Flores MV. Live imaging of Runx1 expression in the dorsal aorta tracks the emergence of blood progenitors from endothelial cells. *Blood.* 2010;116(6):909-14.
 47. Paik EJ, Zon LI. Hematopoietic development in the zebrafish. *Int J Dev Biol.* 2010;54(6-7):1127-37.
 48. Quintana AM, Picchione F, Klein Geltink RI, Taylor MR, Grosveld GC. Zebrafish ETV7 regulates red blood cell development through the cholesterol synthesis pathway. *Disease models & mechanisms.* 2014;7(2):265-70.
 49. Takahashi W, Sasaki K, Kvomatsu N, Mitani K. TEL/ETV6 accelerates erythroid differentiation and inhibits megakaryocytic maturation in a human leukemia cell line UT-7/GM. *Cancer Sci.* 2005;96(6):340-8.
 50. Roukens MG, Allouf-Ramdhani M, Baan B, Kobayashi K, Peterson-Maduro J, van Dam H, et al. Control of endothelial sprouting by a Tel-CtBP complex. *Nature Cell Biol.* 2010;12(10):933-42.